Semicond. Sci. Technol. 10 (1995) 715–719. Printed in the UK

LETTER TO THE EDITOR

Strain-induced magnetoresistance oscillations in GaAs–AlGaAs heterojunctions with ferromagnetic and superconducting submicrometre gratings

P D Ye†, D Weiss†, R R Gerhardts†, K von Klitzing†, K Eberl†, H Nickel‡ and C T Foxon§‖

† Max-Planck-Institut für Festkörperforschung, D-70569 Stuttgart, Germany
‡ Forschungsinstitut der Deutschen Bundespost, D-64295 Darmstadt, Germany
§ Department of Physics, University of Nottingham, Nottingham NG7 2RD, UK

Received 6 March 1995, accepted for publication 13 March 1995

Abstract. We investigated the low-field magnetoresistance ρ_{xx} of a two-dimensional electron gas (2DEG) underneath ferromagnetic and superconducting metallic gratings. The strain due to the different thermal expansion coefficients of the metallic grating and the GaAs–AlGaAs heterojunctions results in a one-dimensional superlattice potential in the plane of the 2DEG. Depending on the aspect ratio of the gratings, different harmonics of the potential can be resolved in ρ_{xx}. The observed resistance anomalies can be modelled in a simple semiclassical model.

The low-temperature resistance of a two-dimensional electron gas (2DEG) subjected to both a weak one-dimensional periodic potential and a perpendicular magnetic field displays oscillations which reflect the commensurability between the classical cyclotron radius R_c (at the Fermi energy E_F) and the period a [1]. Minima then always appear in the resistance when

$$2R_c = (\lambda - \tfrac{1}{4})a \qquad (1)$$

holds, where $\lambda = 1, 2, \ldots$ is an integer oscillation index. The period a, typically of the order of a few hundred nanometres, is much smaller than the electron mean free path ℓ_e, which has a characteristic length of several microns. The imposed periodic potential results in the formation of Landau bands which provide an additional contribution to the resistivity [2, 3]. This contribution vanishes when the Landau bands become flat, i.e. when they have no dispersion with respect to the centre coordinate x_0. This 'flat-band condition' occurs in the case of an *electrostatic* periodic potential when equation (1) holds. Classically, the absence of the additional resistivity contribution corresponds to electrons whose centres of motion do not drift in the periodic potential [4]. These commensurability oscillations emerge in a magnetic field regime where at $T \sim 4.2$ K Shubnikov–de Haas (SdH) oscillations are usually not resolved.

Recently, the transport properties of electrons in a 2DEG subjected to a periodic *magnetic* modulation have attracted a lot of interest [5–12]. Such investigations might also be relevant for a deeper understanding of the motion of composite fermions in the fractional quantum Hall regime in a modulated *effective* magnetic field [13, 14]. Three methods of establishing a periodic magnetic field on the nanometre scale can be envisaged: (i) using periodically arranged flux tubes in a type-II superconductor (Abrikosov lattice) which penetrate the underlying 2DEG, (ii) using patterned superconducting gates which partially shield the external magnetic field or (iii) employing microfabricated ferromagnetic structures whose magnetic polarization adds to the external field. Since the first method is limited to low magnetic fields [15] and, in addition, a *periodic* flux lattice is hardly achievable in an evaporated film, we concentrate on the two latter methods below.

We used periodically arranged niobium and nickel strips on top of a 2DEG to try to establish a one-dimensional (1D) magnetic modulation in the plane of the 2DEG. For this type of modulation distinct theoretical predictions exist for the resistivity ρ_{xx} [6, 8–10]: as in an electrostatic periodic

‖ Samples grown at Philips Research Laboratories, Redhill, UK.

0268-1242/95/050715+05$19.50

potential the energy spectrum can be described in terms of Landau bands which become flat, but when

$$2R_c = (\lambda + \tfrac{1}{4})a \qquad (2)$$

holds. Hence, in a periodic magnetic field ρ_{xx} maxima are expected at magnetic field values where the resistivity of a corresponding electrostatically modulated 2DEG displays minima.

The samples were prepared from conventional GaAs–AlGaAs heterojunctions grown by molecular beam epitaxy. We used different materials which had carrier densities between $n_s = 2.0 \times 10^{11}$ cm^{-2} and 2.8×10^{11} cm^{-2} with mobilities ranging from $\mu = 1.3 \times 10^6$ cm^2 V^{-1}s^{-1} to 1.7×10^6 cm^2 V^{-1}s^{-1}, measured at 4.2 K in the patterned segments of the devices. The corresponding elastic mean free paths are around 12 μm. The distance between the sample surface and the 2DEG for both materials was $\sim$ 100 nm. We also investigated devices made from a lower mobility material where the 2DEG was closer (55 nm) to the surface. Since the basic results were the same we concentrate on the high mobility samples below.

Hall bars, sketched in figure 1(a), were fabricated using optical lithography and subsequent wet chemical etching to define the mesa. Ohmic contacts to the 2DEG were made by alloying AuGe/Ni pads at 450 °C in a reducing atmosphere. 10 nm thick aluminium front gates evaporated on top of the left and the right Hall bar in figure 1(a) allow us to vary the carrier density and define a homogeneous Schottky barrier underneath the gates. On one of the gates nickel or niobium strips were deposited, while the other device served as a reference. We used conventional electron-beam lithographic and lift-off techniques to define the metallic gratings with periods $a = 500$ nm and 950 nm; the height of the strips was about 180 nm. An electron micrograph of a nickel grating with $a = 500$ nm is shown in figure 1(b). The four-point magnetoresistance measurements were performed in a ^{4}He cryostat with superconducting coils by standard lock-in techniques. For all experiments, the magnetic field B was applied normal to the plane of the 2DEG.

Figure 2(a) shows ρ_{xx} measured perpendicular to the niobium grating with period $a = 950$ nm. A pronounced positive magnetoresistance is followed by oscillations. SdH oscillations start to appear at about 0.5 T at 4.2 K. In the presence of a *periodic magnetic field* we expect, according to equation (2), maxima in ρ_{xx} at about 0.2 and 0.085 T (for $\lambda = 1, 2$) with corresponding minima at 0.11 and 0.066 T,

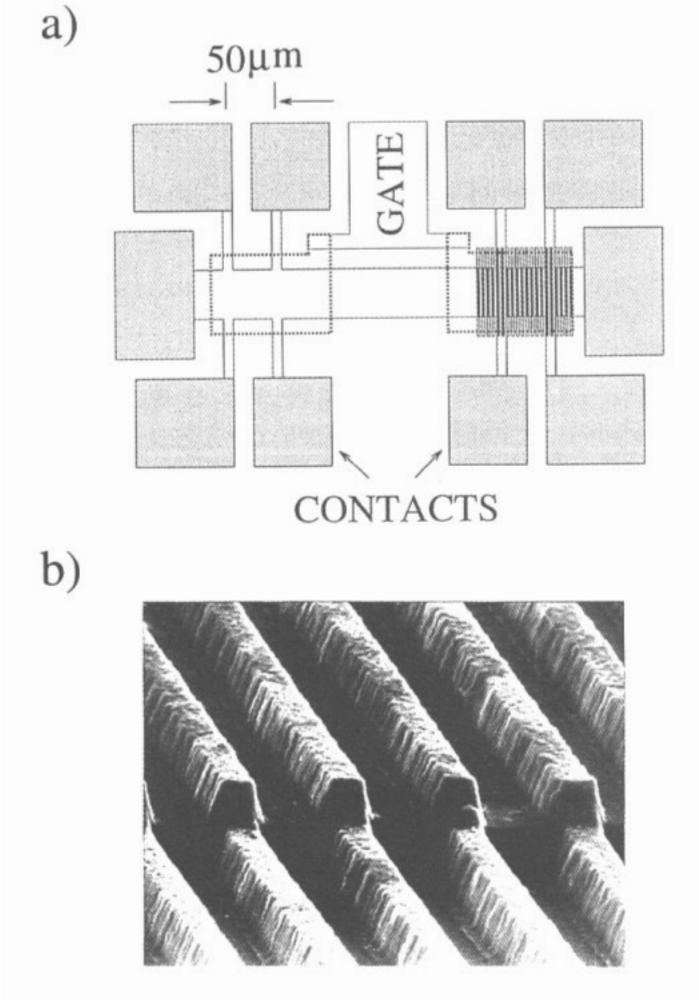

Figure 1. (a) Sketch of the Hall bar geometry containing the grating (right) and an unpatterned reference segment (left). (b) Electron micrograph of a Ni grating with $a = 500$ nm evaporated across a mesa edge. The height of the strips is $\sim$ 180 nm.

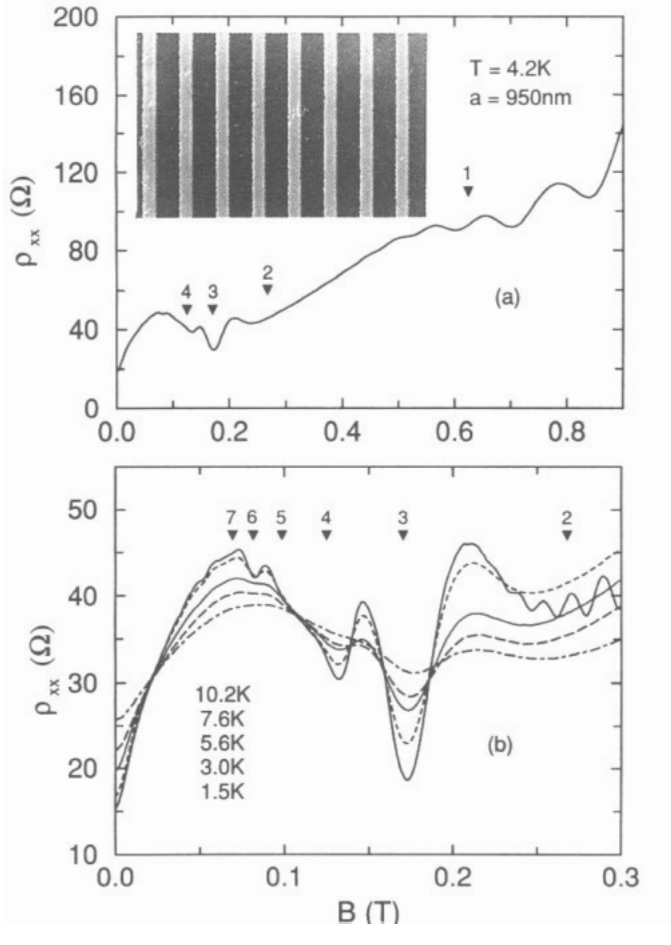

Figure 2. (a) ρ_{xx} measured underneath a Nb grating with $a = 950$ nm. The inset displays an electron micrograph (top view) of the grating (bright strips: niobium) with aspect ratio $w/a \sim 1/3$. (b) Temperature dependence of ρ_{xx}. The triangles in (a) and (b) mark the flat-band positions given by equation (1) for $a/3 \sim 317$ nm.

respectively. While maxima are present at these magnetic field values, the minima are missing. Since in addition the pronounced minima at 0.13, 0.17, 0.25 and 0.7 T remain unexplained in the picture of magnetic modulation, we conclude that the oscillations are not due to a periodic magnetic field. This is evident from figure 2(*b*) where ρ_{xx} is displayed for different temperatures in the low B regime. While the niobium grating is superconducting at 1.5 K, it returns to the normal state above T_c between 4.3 and 6.3 K†. Above T_c the magnetic modulation is expected to be absent. Since the oscillations in ρ_{xx} are present even above T_c, although thermally smeared, they must have a different origin. The oscillations are best described by assuming the presence of a higher harmonic of an *electrostatic* potential modulation with period $a/3 \sim 317$ nm. The corresponding minima predicted by equation (1) are marked by arrows in figures 2(*a*) and (*b*). The fact that every third minimum (i.e. $\lambda = 3, 6$) in figure 2(*b*) is especially strong indicates that the third harmonic dominates in the potential. Inspection of an electron micrograph of the grating in figure 2(*a*) points to the origin of the strong third harmonic in the potential: while the period a of the superlattice is ~ 950 nm, the width w of the niobium strips is only $a/3$. It is obviously the stress at the edges of the strips caused by the different thermal expansion coefficients of GaAs (AlGaAs) and niobium which gives rise to the third harmonic in the potential.

Following this line, we display the resistivity data of a device with aspect ratio $w/a = 250$ nm/500 nm (see inset) in figure 3(*a*). Here, we have used a ferromagnetic nickel grating to generate a magnetic field modulation. As for the device with a superconducting grating, we see no evidence for the presence of a modulated magnetic field. The rich oscillatory structure in figures 3(*a*) and (*b*) at magnetic fields below 1 T can be ascribed to an electrostatic potential modulation with period $a/2 = 250$ nm. Here, even oscillation minima ($\lambda = 2, 4, 6$) are especially deep. It is the strain at the edges of the metallic strips which introduces the second harmonic of the grating period.

A continuous aluminium film underneath the gratings defines an equipotential plane on top of the heterojunction, and hence only strain remains as the origin of the lateral superlattice potential. In a comparable system oscillations with the *fundamental* period of the grating have been found. Also these oscillations were ascribed to strain induced by the heterogeneous material combination [10]. 'Stressors' have been used intentionally in recent work to achieve a lateral confinement of carrier heterojunctions via the deformation potential [17–19]. In a recent paper a theory of potential modulation in lateral surface superlattices was presented [19]. In this work the metallic grating was applied directly to the semiconductor surface. Apart from contributions due to the periodically varying strain, the lateral variations of the gate potential and the surface potential (different work function in gated and ungated parts) also contribute to the total potential modulation in such systems [19]. The elastic strain results from the differing thermal expansion of the evaporated metal and the

† T_c in corresponding unpatterned $\sim$ 150 nm thick niobium films was $\sim$ 9.2 K.

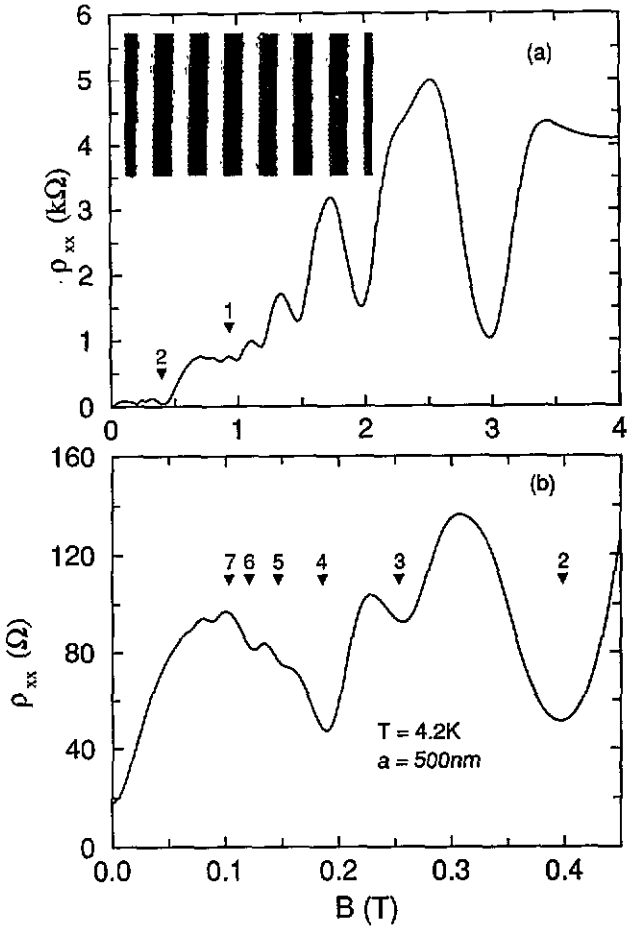

Figure 3. (*a*) High-field and (*b*) low-field magnetoresistance measured underneath a Ni grating with period $a = 500$ nm. The inset in (*a*) displays a top view of the grating with aspect ratio $w/a \sim 1/2$. The flat-band positions for $a/2 \sim 250$ nm are marked by triangles.

GaAs as the sample is cooled to liquid helium temperatures. The metal shrinks by typically a factor 10^{-3} with respect to GaAs at 4.2 K. This results in a compressed region underneath the centre of a metal stripe but regions of expansion near the edges. While the conduction band edge is raised in the contracted region, the potential energy of the electrons is reduced close to the edge of the gate fingers (see figures 4(*a*) and (*b*), top). Typical values of the amplitude of the screened potential modulation are of the order of 1 meV [19].

In order to understand the magnetoresistance oscillations more quantitatively, we model the stress-induced potential landscape within one unit cell of the superlattice by the superposition of three Gaussians: one Gaussian with amplidude V_z and width d describes the potential in the compressed region underneath the stripe, while two Gaussians at the edges with (negative) amplitude V_s and halfwidth b model the potential slope at the edges. This results in a shape of the potential modulation similar to the one calculated in recent work [19]. Then the potential is expanded in a Fourier series

$$V(x) = V_0 + \sum_{n=1}^{\infty} V_n \cos(nkx)$$

with $k = 2\pi/a$ and the coefficients

$$V_n = -4\sqrt{\pi}V_s(b/a)\{\exp[-(n\pi b/a)^2]\cos nkx_0 - (V_z d/2bV_s)\exp[-(n\pi d/a)^2]\}.$$

Next, we calculate the magnetoresistance in such a potential landscape. The magnetoresistance oscillations in a weak *sinusoidal* periodic potential can be described in a classical picture developed by Beenakker, which is based on the guiding-centre drift of the cyclotron orbits [4]. A corresponding classical formula for the resistivity in a weak periodic potential of *arbitrary shape* can be found in reference [20],

$$\frac{\Delta\rho_{xx}}{\rho_0} = 4\left(\frac{V_s}{E_F}\right)^2\left(\frac{\ell_e}{a}\right)^2\frac{a}{R_c} \times \sum_{n=1}^{\infty} n\left|\frac{V_n}{V_s}\right|^2 \cos\left(2\pi n\frac{R_c}{a} - \frac{\pi}{4}\right) \qquad (3)$$

where $\Delta\rho_{xx} = \rho_{xx} - \rho_0$ with the zero-field resistivity ρ_0 of the unpatterned 2DEG and E_F is the Fermi energy.

The result of such calculations is shown in figure 4. Figures 4(*a*) and (*c*) display the shapes of the conduction band edge used to model the magnetoresistance underneath the niobium and nickel grating, respectively. The location of the gate is indicated by a black bar. Figures 4(*b*) and (*d*) show the change in the magnetoresistance $\Delta\rho_{xx}$ obtained from equation (3) using the model potentials displayed above. The calculated traces nicely reproduce the dominating features of figures 2 and 3. In $\Delta\rho_{xx}$ of figure 4(*b*) the third harmonic of the periodic potential dominates, as a consequence of the aspect ratio $w/a \sim 1/3$. The fact that every third minimum is especially deep closely resembles the experimental data of figures 2(*a*) and (*b*). The triangles in figure 4(*b*) mark the flat-band condition of the third harmonic obtained by using $a/3$ instead of a in equation (1). The calculated resistivities for an aspect ratio of $w/a \sim 1/2$, corresponding to the experimental data of figure 3, are displayed in figure 4(*d*). As in experiment, the calculated ρ_{xx} trace exhibits pronounced minima for even values of λ, indicating the influence of the second harmonic. The relative depths of the ρ_{xx} minima depend sensitively on the ratio V_z/V_s and the half-widths of the Gaussians that model the strain. A slight change in these parameters, as is displayed in figure 4(*c*), results in figure 4(*d*) in either a dominating fundamental (chain curve) or second (broken curve) harmonic in $\Delta\rho_{xx}$.

In summary, we have shown that the strain connected with patterened gates results in a periodic potential which can lead to pronounced *electric* commensurability effects and can thus prevent the observation of effects related to a periodic *magnetic* field. In contrast to previous work the strain-induced deformation potential is the only source of the electrostatic modulation. During the preparation of this manuscript both we and others [22, 23] succeeded in observing effects from a periodic magnetic field by using either patterned ferromagnetic [21, 23] or superconducting [22] gates. To overcome the stress problem either the saturation magnetization of the ferromagnetic material can be increased by using dysprosium [21] or the strain underneath a gate finger can be reduced by applying a positive bias to the nickel grating, which increases the carrier density locally [23].

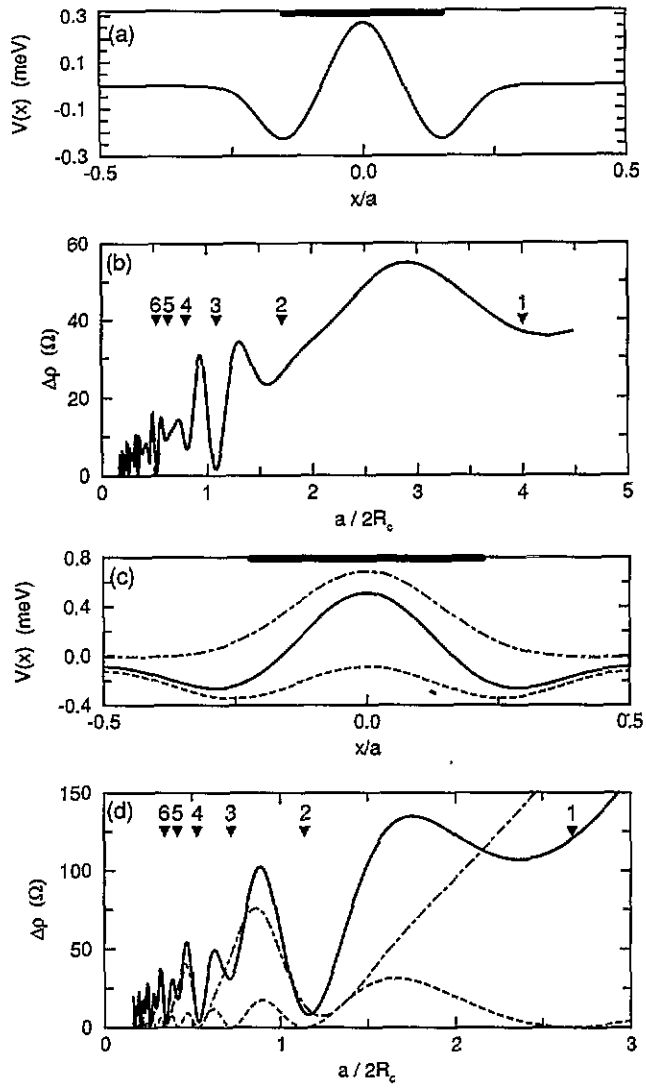

Figure 4. (*a*) The potential slope used to simulate the conduction band edge underneath the Nb grating with $w/a \sim 1/3$. The black bar at the top indicates the gate position. The corresponding resistance trace obtained from equation (3) is displayed in (*b*). The flat-band positions for the third harmonic are indicated by triangles. (*c*) Potential slope modelling the situation underneath our Ni grating with $w/a \sim 1/2$ (full curve). The corresponding resistance trace in (*d*) exhibits the characteristic features displayed by the data of figure 3. Changes in the model potential (broken and chain curves in (*c*)) significantly affect the corresponding $\Delta\rho_{xx}$ traces in (*d*).

We would like to thank M Riek and A Gollhardt for their expert help in processing the samples, and G H Li, G Lütjering and M Tornow for valuable discussions. P D Ye acknowledges the Volkswagen Foundation for fellowship.

References

[1] Weiss D, von Klitzing K, Ploog K and Weimann G 1989 *Europhys. Lett.* **8** 179; see also *High Magnetic Fields in Semiconductor Physics II (Springer Series in Solid State Sciences 87)* ed G Landwehr (Berlin: Springer) p 357

[2] Gerhardts R R, Weiss D and von Klitzing K 1989 *Phys. Rev. Lett.* **62** 1173
[3] Winkler R W, Kotthaus J P and Ploog K 1989 *Phys. Rev. Lett.* **62** 1177
[4] Beenakker C W J 1989 *Phys. Rev. Lett.* **62** 2020
[5] Yoshioko D and Iye Y 1987 *J. Phys. Soc. Japan* **56** 488
[6] Vasilopoulos P and Peeters F M 1990 *Superlatt. Microstruct.* **7** 393
[7] Wu X and Ulloa S E 1992 *Solid State Commun.* **82** 945
[8] Peeters F M and Vasilopoulos P 1993 *Phys. Rev.* B **47** 1466
[9] Xue D P and Xiao G 1992 *Phys. Rev.* B **45** 5986
[10] Yagi R and Iye Y 1993 *J. Phys. Soc. Japan* **62** 1279
[11] Schmidt G J O 1993 *Phys. Rev.* B **47** 13007
[12] Schmelcher P and Shepelyansky D L 1994 *Phys. Rev.* B **49** 7481
[13] Kang W, Störmer H L, Pfeiffer L N, Baldwin K W and West K W 1993 *Phys. Rev. Lett.* **71** 3850
[14] Willet R L, Ruel R R, West K W and Pfeiffer L N 1993 *Phys. Rev. Lett.* **71** 3846
[15] Bending S J, von Klitzing K and Ploog K 1990 *Phys. Rev. Lett.* **65** 1060
[16] Kash K, Worlock J M, Mahoney D D, Gozdz A S, Van der Gaag B P, Harbison J P, Lin P S D and Florez L T 1987 *Surf. Sci.* **146** 27
[17] Kash K, Bhat R, Mahoney D D, Lin P S D, Scherer A, Worlock J M, Van der Gaag B P, Koza M and Grabbe P 1989 *Appl. Phys. Lett.* **55** 681
[18] Kash K, Van der Gaag B P, Mahoney D D, Gozdz A S, Florez L T, Harbison J P and Sturge M D 1991 *Phys. Rev. Lett.* **67** 1326
[19] Davies J H and Larkin I A 1994 *Phys. Rev.* B **49** 4800
[20] Gerhardts R R 1992 *Phys. Rev.* B **45** 3449
[21] Ye P D, Weiss D, Gerhardts R R, Seeger M, von Klitzing K, Eberl K and Nickel H 1995 *Phys. Rev. Lett.* to be published
[22] Carmona H A, Geim A K, Nogaret A, Foster T J, Main P C, Beaumont S P and Blamire M G *Preprint*
[23] Izawa S, Katsumot S, Endo A and Iye Y *Preprint*